ORIGINAL RESEARCH ARTICLE

Development and Evaluation of a Virtual Population of Children with Obesity for Physiologically Based Pharmacokinetic Modeling

Jacqueline G. Gerhart[1] · Fernando O. Carreño[1] · Andrea N. Edginton[2] · Jaydeep Sinha[1] · Eliana M. Perrin[3] ·
Karan R. Kumar[4,5] · Aruna Rikhi[4] · Christoph P. Hornik[4,5] · Vincent Harris[1] · Samit Ganguly[1,6] ·
Michael Cohen-Wolkowiez[4,5] · Daniel Gonzalez[1] 🄳 on behalf of the Best Pharmaceuticals for Children Act—
Pediatric Trials Network Steering Committee

Abstract

Background and Objective While one in five children in the USA are now obese, and more than three-quarters receive at least one drug during childhood, there is limited dosing guidance for this vulnerable patient population. Physiologically based pharmacokinetic modeling can bridge the gap in the understanding of how pharmacokinetics, including drug distribution and clearance, changes with obesity by incorporating known obesity-related physiological changes in children. The objective of this study was to develop a virtual population of children with obesity to enable physiologically based pharmacokinetic modeling, then use the novel virtual population in conjunction with previously developed models of clindamycin and tri-methoprim/sulfamethoxazole to better understand dosing of these drugs in children with obesity.

Methods To enable physiologically based pharmacokinetic modeling, a virtual population of children with obesity was developed using national survey, electronic health record, and clinical trial data, as well as data extracted from the literature. The virtual population accounts for key obesity-related changes in physiology relevant to pharmacokinetics, including increased body size, body composition, organ size and blood flow, plasma protein concentrations, and glomerular filtration rate. The virtual population was then used to predict the pharmacokinetics of clindamycin and trimethoprim/sulfamethoxazole in children with obesity using previously developed physiologically based pharmacokinetic models.

Results Model simulations predicted observed concentrations well, with an overall average fold error of 1.09, 1.24, and 1.53 for clindamycin, trimethoprim, and sulfamethoxazole, respectively. Relative to children without obesity, children with obesity experienced decreased clindamycin and trimethoprim/sulfamethoxazole weight-normalized clearance and volume of distribution, and higher absolute doses under recommended pediatric weight-based dosing regimens.

Conclusions Model simulations support current recommended weight-based dosing in children with obesity for clindamycin and trimethoprim/sulfamethoxazole, as they met target exposure despite these changes in clearance and volume of distribution.

1 Introduction

Childhood obesity is an alarming public health threat, with obesity rates nearly quadrupling in children aged 2–19 years in the past quarter-century. Almost one in five children in the USA, and 8.7% worldwide, are obese [1–3]. Compared

✉ Daniel Gonzalez
daniel.gonzalez@unc.edu

Extended author information available on the last page of the article

to their normal-weight counterparts, children with obesity experience higher rates and severity of multiple disease states and require significantly more prescriptions [4, 5]. Obesity is known to influence the pharmacokinetics (PK) of many drugs because of the effect of altered body size (including body composition) on drug distribution and elimination. Thus, dosing for children with obesity must account for the effect of obesity on PK [6–9]. One systematic review of clinical studies conducted in children with obesity found clinically significant pharmacokinetic alterations in 65% of drugs studied, with changes in the weight-normalized volume of distribution and clearance varying between drugs [10]. Despite the high prevalence of childhood obesity and

Key Points

Childhood obesity is an alarming public health threat, with obesity rates nearly quadrupling in children aged 2–19 years in the past quarter-century and almost one in five children classified as obese in the USA today.

To enable physiologically based pharmacokinetic modeling to better characterize the exposure of drugs in a growing number of children with obesity, a virtual population of children with obesity was developed for multiple racial groups that accounts for key obesity-related physiological changes affecting pharmacokinetics, including increased body size, organ size and blood flow, plasma protein concentrations, and glomerular filtration rate.

This novel virtual population of children with obesity was used with previously developed pediatric physiologically based pharmacokinetic models of clindamycin and trimethoprim/sulfamethoxazole to characterize exposure of these drugs. Physiologically based pharmacokinetic model dosing simulations suggest that, despite higher exposure from decreased weight-normalized clearance and volume of distribution, recommended weight-based dosing of clindamycin and trimethoprim/sulfamethoxazole is adequate for children with obesity.

its impact on drug exposure, children with obesity remain understudied. This patient subgroup is particularly challenging to study clinically, as stigma can further lower pediatric enrollment rates, making it challenging to include the full age and body size range of children required to characterize drug disposition. As a result, few US Food and Drug Administration (FDA) labels provide dosing guidance in this population [11].

Physiologically based pharmacokinetic (PBPK) modeling can account for obesity-related changes in physiology to characterize altered drug disposition in children with obesity. Physiologically based pharmacokinetic modeling integrates physiological variables (e.g., organ size and blood flow) into a virtual population, then adds drug-related properties (e.g., physicochemical and metabolism characteristics) and study design elements (e.g., dosing and sampling times) to predict drug disposition and inform dosing mechanistically [12, 13]. A virtual population of children used in PBPK modeling offers advantages over traditional population pharmacokinetic methods by (1) characterizing developmental and obesity-related physiological changes in children to capture the effect of both age and body size on drug disposition, (2) predicting initial PK in children with

obesity in the absence of any yet available clinical data, and (3) incorporating mechanistic information required to understand differences in PK [14]. This approach has been successfully used previously when a virtual population of adults with obesity was developed and used to predict the clearance of eight drugs in adults [15]. However, there currently is no virtual population developed for children with obesity and thus no PBPK models for these children.

This study aimed to extend an existing virtual pediatric population to reflect the obesity-related physiological changes in children to enable PBPK modeling for this vulnerable population [16]. Existing data were leveraged from multiple sources, including previously reported literature, national surveys, electronic health records, and clinical studies of children with and without obesity to incorporate all known relevant obesity-related physiological changes to predict PK. This new virtual population was evaluated by expanding previously developed pediatric PBPK models of clindamycin and trimethoprim/sulfamethoxazole to include observed data from children with obesity [17, 18]. Clindamycin and trimethoprim/sulfamethoxazole were chosen because of the availability of extensive on-hand individual concentration data, and they are extensively prescribed to children with obesity. PBPK model simulations were used to determine potential dosing adjustments necessary for children with obesity to attain known target exposure.

2 Methods

2.1 Data Sources for Virtual Population Development

Demographic data, including body weight, body mass index (BMI), race, and ethnicity, as well albumin data, were obtained from the US Centers for Disease Control and Prevention (CDC) National Health and Nutrition Examination Survey (NHANES) from 1999 to 2016 (Table 1) [19]. Further demographic and albumin concentration data were obtained from the Pediatric Trial Network (PTN) Data Repository, a data warehouse containing electronic health records for ~ 265,000 pediatric patients across nine US hospitals [20]. Albumin and α1-acid glycoprotein (AAG) concentrations were available from clinical trials enrolling children with and without obesity, including the 'Safety and Pharmacokinetics of Clindamycin in Pediatric Subjects with BMI ≥ 85th Percentile' (CLIN01, ClinicalTrials.gov #NCT01744730), 'Pharmacokinetics of Multiple Dose Methadone in Children Treated for Opiate Withdrawal' (MTH01, ClinicalTrials.gov #NCT01945736), and 'Pharmacokinetics of Understudied Drugs Administered to Children Per Standard of Care' (POP01, ClinicalTrials.gov #NCT01431326) studies [21, 22]. To incorporate existing

physiological data from children with obesity into our virtual population, a comprehensive literature search was conducted in PubMed for physiological terms relevant to PK. Detailed search methods are included in Sect. 1.1 of the Electronic Supplementary Material (ESM).

2.2 Inclusion Criteria

Children aged 2–20 years were included in this analysis, in-line with the CDC's definition of pediatric obesity. Children with a BMI ≥ 95th percentile were considered obese, as defined by the 2000 CDC growth charts [23]. Available

data from all reported races and ethnicities of children with obesity were used to inform the virtual population.

2.3 PBPK Modeling

Pediatric PBPK models of clindamycin and trimethoprim/sulfamethoxazole previously developed in PK-Sim® (version 9.0; Open Systems Pharmacology Suite, open-systems—pharmacology.org) for children without obesity were used with the virtual population to simulate observed plasma concentrations in real-world children with obesity [17, 18].

Table 1 Population demographics for pediatric subjects with and without obesity from the National Health and Nutritional Examination Survey (NHANES) [pooled data from 1999 to 2016], the Pediatric Trials Network (PTN) data repository, and combined drug trial datasets

Demographics[a]	NHANES		PTN data repository		Combined drug trials	
	Obese	Nonobese	Obese	Nonobese	Obese	Nonobese
n, subjects	6725	27,410	13,747	62,511	412	292
Age, years	12.3 (2.0, 21.1)	11.0 (2.0, 21.1)	11.5 (2.0, 17.0)	10.2 (2.0, 17.0)	13.1 (2.1, 20.2)	12.7 (2.0, 20.6)
Weight, kg	69.3 (13.9, 239.4)	37.5 (8.9, 110.4)	64.6 (10.9, 655.0[b])	31.3 (10.0, 114.0)	70.3 (11.3, 164.4)	36.6 (8.1, 101.6)
Height, cm	146.6 (83.2, 197.2)	144.8 (79.0, 204.0)	150.0 (75, 206.0)	138.0 (75.0, 211)	152.2 (48.4, 193.0)	143.0 (75.5, 195.0)
BMI, kg/m²	28.2 (17.9, 73.4)	17.9 (8.0, 31.7)[c]	28.0 (17.8, 258.5[b])	17.1 (4.8, 29.6)	29.4 (18.1, 62.1)	17.6 (11.0, 31.3)[c]
BMI percentile, %[d]	98.2 (95.0, 100.0)	60.9 (0, <95.0)	98.3 (95.0, 100.0)	52.8 (0, <95.0)	98.6 (95.0, 100.0)	50.2 (0, 95.0)
Male	3472 (51.6%)	13,798 (50.3%)	7102 (51.7%)	31,180 (49.9%)	231 (56.1%)	150 (51.4%)
Race						
American Indian/ Alaskan Native	NR	NR	103 (0.7%)	254 (0.4%)	2 (0.5%)	1 (0.3%)
Asian	105 (1.6%)	911 (3.3%)	215 (1.6%)	1932 (3.1%)	4 (1.0%)	7 (2.4%)
Black or African American	2026 (30.1%)	7521 (27.4%)	2987 (21.7%)	11,512 (18.4%)	61 (14.8%)	57 (19.5%)
Mexican American	2209 (32.8%)	7431 (27.1%)	NR	NR	NR	NR
Multiple races	NR	NR	358 (2.6%)	1230 (2.0%)	14 (3.4%)	11 (3.8%)
Native Hawaiian/ Pacific Islander	NR	NR	54 (0.4%)	210 (0.3%)	4 (1.0%)	0
Other	NR	NR	1520 (11.1%)	5107 (8.2%)	1 (0.2%)	0
Other Hispanic	596 (8.9%)	2097 (7.7%)	NR	NR	NR	NR
White	1473 (21.9%)	7904 (28.8%)	7658 (55.7%)	38,461 (61.5%)	306 (74.3%)	208 (71.2%)
Unknown/NR	316 (4.7%)	1546 (5.6%)	852 (6.2%)	3805 (6.1%)	20 (4.9%)	8 (2.7%)
Ethnicity						
Hispanic/Latino	NR	NR	4109 (29.9%)	13,419 (21.5%)	86 (20.9%)	49 (16.8%)
Not Hispanic/ Latino	NR	NR	9169 (66.7%)	46,503 (74.4%)	318 (77.2%)	238 (81.5%)
Unknown/NR	NR	NR	469 (3.4%)	2589 (4.1%)	8 (1.9%)	5 (1.7%)

Values are medians (range) for continuous variables and counts (%) for categorical variables

BMI body mass index, *CDC* Centers for Disease Control and Prevention, *NR* not reported in the dataset

[a]Demographics recorded at the time of the first study dose were used to calculate descriptive statistics

[b]Note that one observed child with obesity in the PTN data repository dataset had an extremely high weight recorded (655.0 kg) that may be due to a recording error

[c]Note that while the maximum BMI for children without obesity exceeds the adult cut-off for obesity (BMI ≥ 30 kg/m²), these children had a BMI percentile ≤ 95, just missing the CDC's pediatric cut-off for obesity

[d]BMI percentile was calculated using the 2000 CDC growth charts. Children with a BMI ≥ 95th percentile were considered obese

2.3.1 Clinical Data

For both the clindamycin and trimethoprim/sulfamethoxazole PBPK models, clinical data from children with obesity from the POP01 and the External Data Study were used [24–26]. The External Data Study was a multicenter, open-label, interventional pharmacokinetic and safety study as previously described for trimethoprim/sulfamethoxazole [26]. Clindamycin data from the External Data Study have not previously been published and are described in more detail in Sect. 1.5 of the ESM. Additional data were used from the CLIN01 study to evaluate the clindamycin PBPK model [21]. A summary of clinical studies used in this work is shown in Table 1 of the ESM, and demographics of all subjects are shown in Tables 2, 3, 4 and 5 of the ESM.

2.3.2 PBPK Model Development

As previously described, a PBPK model of clindamycin was developed in adults (without obesity) incorporating conversion of the clindamycin phosphate dose to active clindamycin via alkaline phosphatase, clindamycin metabolism via cytochrome P450 (CYP) 3A4 and 3A5, and excretion via tubular secretion and glomerular filtration [17]. The clindamycin model was scaled and evaluated in children (without obesity) using known ontogeny functions for AAG, alkaline phosphatase, CYP3A4, CYP3A5, and renal function [17]. A PBPK model of trimethoprim/sulfamethoxazole was developed in adults as previously described [18]. The trimethoprim model incorporated CYP2C9-mediated and CYP3A4-mediated metabolism and renal elimination via tubular secretion and glomerular filtration [18]. The sulfamethoxazole model incorporated CYP2C9-mediated and N-acetyl transferase 2 (NAT2)-mediated metabolism and renal elimination via glomerular filtration [18]. The models were scaled and evaluated in children without obesity using known ontogeny functions for AAG, albumin, CYP2C9, CYP3A4, CYP3A5, NAT2, and renal function [18]. Final scaled clindamycin and trimethoprim/sulfamethoxazole model parameters are shown in Tables 6 and 7 of the ESM.

2.3.3 PBPK Model Evaluation

Because subjects experienced wide inter-individual variations in dosing (both amount and frequency), it was not possible to simulate the concentrations of all subjects together in a population-based simulation. Therefore, simulations were performed for each subject using "individualized" virtual populations ($n = 200$) matched to that particular subject's demographics and dosing. Simulations were evaluated by calculating the number of observed concentrations falling within the 90% model prediction interval. PBPK predictions were also evaluated by average fold error (AFE) of

the observed to the median simulated concentration for all samples using the equation:

$$\text{AFE} = 10^{\frac{1}{n} \sum \log \left(\frac{\text{predicted}}{\text{observed}} \right)} \tag{1}$$

where n is the total number of samples. An AFE within a 0.5-fold to two-fold error was considered an acceptable model fit.

2.3.4 PBPK Model Dosing Simulations

Population simulations were performed using the newly developed virtual population to understand how well current recommended pediatric dosing of the aforementioned drugs results in target exposure achievement in children with obesity. Virtual populations of 1000 children with obesity were created for each age group (Table 8 of the ESM).

For clindamycin, recommended dosing of a 12 mg/kg intravenous infusion (30 minutes) for children aged > 2–6 years and 10 mg/kg intravenously for children aged > 6–18 years was simulated [17, 25]. Target achievement was defined as median steady-state area under the concentration–time curve from 0 to 8 h ($\text{AUC}_{0-8,\text{ss}}$) within 25% of the median $\text{AUC}_{0-8,\text{ss}}$ of adults receiving the recommended reference dose of 600 mg intravenously [27]. Dose capping was implemented using the maximum FDA-recommended intravenous dose of 900 mg [11].

For trimethoprim/sulfamethoxazole, recommended coadministration of trimethoprim 6 mg/kg and sulfamethoxazole 30 mg/kg orally (PO) for children aged > 2–12 years and trimethoprim 4 mg/kg and sulfamethoxazole 20 mg/kg for children aged > 12–18 years was simulated [18, 28]. Trimethoprim target attainment was defined as > 80% of virtual children exceeding an adult reference steady-state area under the concentration–time curve (AUC_{ss}) of 20.6 mg * h/L, and > 95% of children falling below safety margins for trimethoprim (13.6 mg/L maximum concentration, 141.8 mg * h/L AUC_{ss}) and sulfamethoxazole (372 mg/L maximum concentration, 4119.4 mg * h/L AUC_{ss}) [29]. Dose capping was implemented using the maximum FDA-recommended dosing of 320 mg for trimethoprim and 1600 mg for sulfamethoxazole [30]. A fixed adult dose of 600, 160, and 800 mg was also simulated for clindamycin, trimethoprim, and sulfamethoxazole, as again many observed children with obesity received fixed adult doses.

3 Results

3.1 Body Size

While the CDC's obesity definition is a BMI ≥ 95th percentile, the prevalence of obesity has increased significantly

since the 1980s, when data for the 2000 CDC growth charts were collected. There is an upward shift in BMI for current children such that a greater number of children are above the CDC-defined obesity cut-off. To create a virtual population of children with obesity that reflects today's higher BMI ranges, the growth curves were updated using more recent data reported in NHANES (Fig. 1). These growth curves were generated using the same lambda-mu-sigma parameter method used for the 2000 CDC growth charts [31]. Separate male and female growth curves were generated for Asian-American, Black-American, Mexican-American, and White-American children (Fig. 1 of the ESM). BMI-for-age data for all three racial groups included in the PTN Data Repository were used to validate the growth curves (Fig. 2 of the ESM). Additional details and final lambda-mu-sigma parameter files can be found in Sect. 1.3 of the ESM.

3.2 Hematocrit

Simulated hematocrit values for virtual children with obesity reflected reported values (0.38–0.43 L/L) in real-world children with obesity (Fig. 3 and Table 9 of the ESM). Further comparison of 136 subjects from trial data showed no significant change in hematocrit across a wide BMI range. Thus, no additional changes in hematocrit with obesity were included in the virtual population.

3.3 Protein Binding

Comparison of albumin concentrations between children with and without obesity from NHANES ($n = 14,293$),

PTN Data Repository ($n = 3,193$), trial data ($n = 393$), and reported values (3.3–4.9 g/dL) showed no observable difference across a wide BMI range (Fig. 4 and Table 10 of the ESM). Comparison of 148 subjects from trial data and reported values in children with obesity (0.8–1.05 g/L) showed no significant change in AAG concentrations across a wide BMI range (Fig. 5 and Table 11 of the ESM). Accordingly, no additional changes in albumin or AAG concentrations with obesity were incorporated into the virtual population.

3.4 Organ Volumes

Organ size increases in children with obesity were implemented in the virtual population by multiplying the organ volumes of virtual children without obesity by an organ-specific scaling factor. Identifying these scaling factors was difficult, as organ volume data in children with obesity in the literature are sparse. Therefore, scaling factors were first derived from an adult study comparing organ volumes of subjects with vs without obesity (Table 12 of the ESM) [32]. Organ size increases from ultrasound measurements of the kidney (median [range] 119% [110–139%]) and liver (118% [105–149%]) in children with vs without obesity were in-line with adult increases of 115% for both the kidney and liver (Fig. 6 and Table 13 of the ESM). After accounting for increases in non-fat organs based on these scaling factors, remaining excess body weight (as determined from the updated growth curves) was attributed to the adipose organ. Because of a lack of composition data in children with obesity (e.g., percent lipids, protein, and water within an organ),
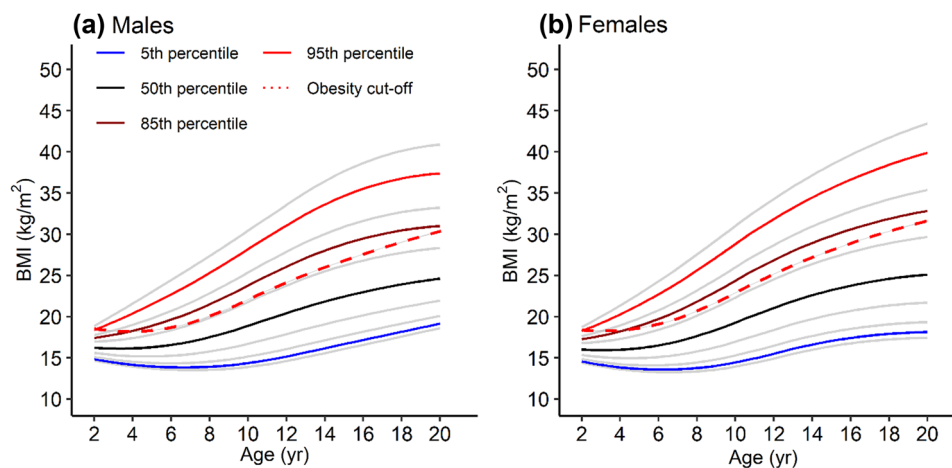
Fig. 1 Updated growth curves based on National Health and Nutrition Examination Survey (NHANES) pooled data for male and female groups. Key body mass index (BMI) percentiles are highlighted in blue (5th percentile), black (50th percentile), dark red (85th percentile), and red (95th percentile). The BMI cut-off for obesity as defined by the Centers for Disease Control and Prevention (CDC) is represented by the bold red dashed line, such that children with a BMI above that line for a given age are considered obese. Files with lambda-mu-sigma (LMS) parameters for plotting the updated growth curves and calculating updated BMI percentiles are provided in the ESM

organ composition was modeled the same way as in existing virtual children without obesity in PK-Sim® [16].

3.5 Body Fat and Fat-Free Mass

To further evaluate the distribution of excess body weight between adipose and lean organs in virtual children with obesity after incorporating organ volume scaling factors, simulated adipose volume was compared to calculated fat mass for virtual children using previously developed fat mass equations [33, 34]. Simulated adipose volume was similar to calculated fat mass, with some overestimation at higher weights that was also observed in the baseline population of virtual children without obesity (Fig. 2).

3.6 Cardiac Output and Organ Blood Flow

Organ blood flows in children with obesity were not available in the literature, thus organ blood flows (in mL/min/kg organ) in virtual children without obesity were retained for children with obesity. However, increasing organ volumes in virtual children with obesity increased absolute blood flow

(in mL/min) depending on the organ size (Fig. 7a of the ESM). Simulated cardiac output (an aggregate measure of blood flow to all perfused organs) was compared to reported values for children with obesity (Fig 7b and Table 14 of the ESM). While the cardiac output widely varied in the literature (4.4–7.3 L/min), the reported cardiac output was similar to simulated values for age.

3.7 Renal Function

As glomerular filtration rate (GFR) is a function of kidney size, increasing kidney volume for children with obesity resulted in elevated absolute GFR. Absolute and size-normalized GFR (mL/min/kg) for virtual children with obesity was in-line with a previously reported study that estimated GFR by measuring creatinine clearance in children with obesity, albeit with more variability (Table 2) [35].

3.8 Drug-Metabolizing Enzymes and Transporters

Although there is some evidence of obesity-related alterations in in vitro activity of key metabolic and transport

Fig. 2 Simulated vs calculated fat mass for 1500 virtual children without (**a** and **c**) and 1500 virtual children with (**b** and **d**) obesity. Simulated fat mass was determined from the volume of the adipose organ generated for each virtual child in PK-Sim®. Calculated fat mass was determined using each virtual child's demographic information and the fat mass equations derived from Al-Sallami et al. (**a** and **b**) and Green et al. (**c** and **d**) [33, 34]. Each point represents a single virtual child. Dashed lines represent the lines of unity for reference, and blue lines represent a linear regression passing through the origin for better visualization of misspecification. The slope of this regression line is 1.26, 1.22, 1.20, and 1.18 for (**a**–**d**), respectively
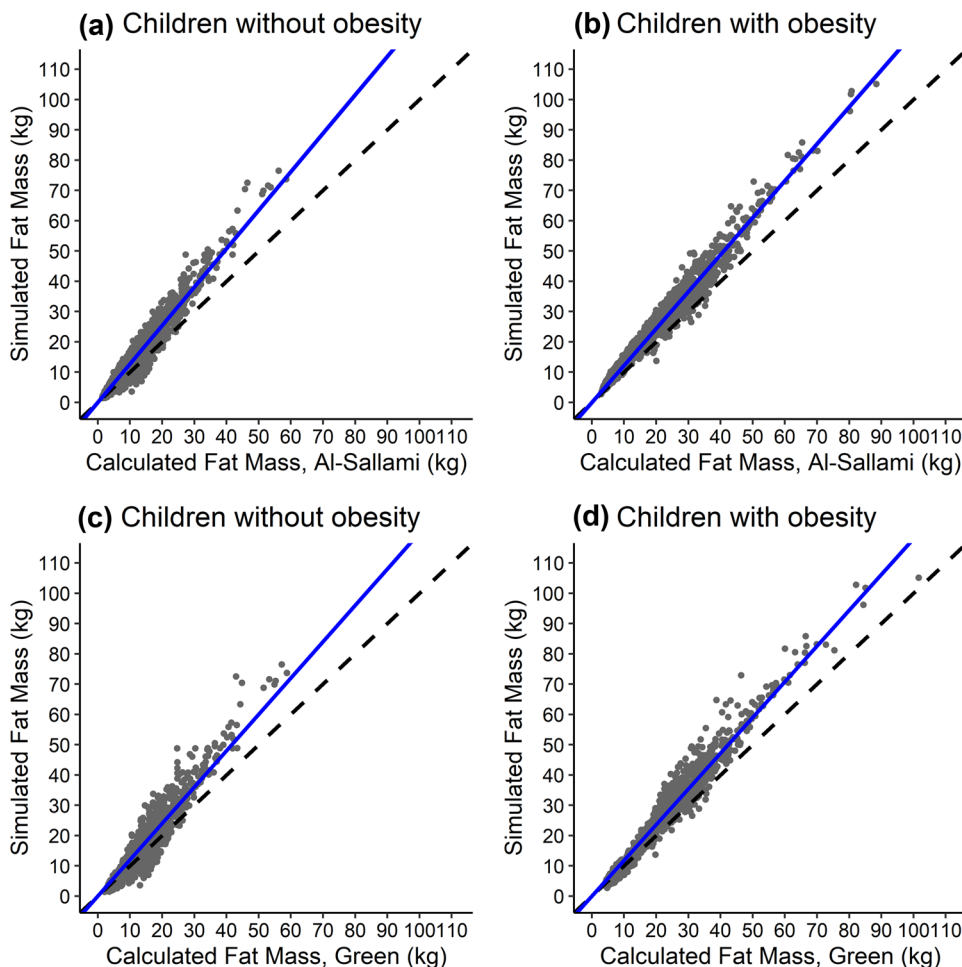
enzymes in adults, such evidence is lacking in children with obesity [36, 37]. Few clinical studies are reported in children with obesity determining changes in metabolism using in vivo data, and those that exist conflict with known changes in adults with obesity [38], possibly owing to lower rates of comorbidities in children. Thus, no changes with obesity were incorporated in virtual children with obesity a priori.

3.9 PBPK Model Development and Evaluation

Validating the original, nonobese clindamycin PBPK model with a secondary dataset including 16 children without obesity with 88 samples collected in the External Data Study resulted in an AFE of 0.74. After adjusting the fraction unbound based on the observed AAG concentration (see Sect. 2.3 of the ESM), expanding the model to include 101 children with obesity ($n = 188$ samples) resulted in 77%

of observed concentrations falling within the 90% model prediction interval (7% above, 16% below), and an AFE of 1.09 (Fig. 8 of the ESM).

The trimethoprim model also captured observed concentrations ($n = 50$) from eight children without obesity well in the secondary validation dataset, with 82% of observed concentrations falling within the 90% model prediction interval (18% above), and an AFE of 1.29 (Fig. 9 of the ESM). Ninety percent of sulfamethoxazole concentrations from children without obesity fell within the 90% model prediction interval (10% above), with an AFE of 1.44 (Fig. 10 of the ESM). Of 50 children with obesity ($n = 87$ trimethoprim and 89 sulfamethoxazole samples), 75% of observed trimethoprim concentrations fell within the 90% model prediction interval (3% above, 22% below), with an AFE of 1.24 (Figs. 11 and 12 of the ESM). Sulfamethoxazole observed concentrations in children with obesity were moderately well captured, with 54% falling with the 90% model

Table 2 Simulated vs reported glomerular filtration rate (GFR) values for children aged 8–9 years with and without obesity

Estimation methods[a]	Nonobese		Obese		Obese/nonobese (%)	
	Reported [35]	Simulated	Reported [35]	Simulated	Reported [35]	Simulated
Absolute (mL/min)		65.0 (21.7)		73.3 (24.7)		112.8
CrCl	93.2 (21.0)		120.8 (21.5)		129.1	
GFR, Zappitelli	79.8 (10.5)		100.1 (14.4)		125.4	
GFR, Schwartz	65.1 (8.3)		83.2 (12.5)		127.8	
Weight-adjusted (mL/min/kg)		1.92 (0.68)		1.64 (0.59)		85.4
CrCl	3.4 (0.7)		2.8 (0.5)		82.4	
GFR, Zappitelli	2.9 (0.4)		2.3 (0.2)		79.3	
GFR, Schwartz	2.4 (0.3)		1.9 (0.2)		79.2	
BMI-adjusted (mL/min/kg/m^2)		3.54 (1.32)		3.03 (1.07)		85.6
CrCl	5.8 (1.4)		5.2 (1.0)		89.7	
GFR, Zappitelli	5.0 (0.7)		4.3 (0.5)		86.0	
GFR, Schwartz	4.1 (0.5)		3.6 (0.4)		87.8	
LBM-adjusted (mL/min/kg)		2.33 (0.78)		2.20 (0.77)		94.4
CrCl	3.9 (0.8)		3.7 (0.6)		94.9	
GFR, Zappitelli	3.4 (0.4)		3.0 (0.3)		88.2	
GFR, Schwartz	2.7 (0.3)		2.5 (0.2)		92.6	
FFM-adjusted (mL/min/kg)		2.56 (0.85)		2.44 (0.85)		95.3
CrCl	4.6 (1.0)		5.0 (0.9)		108.7	
GFR, Zappitelli	3.9 (0.6)		4.1 (0.6)		105.1	
GFR, Schwartz	3.2 (0.5)		3.4 (0.5)		106.3	
BSA-adjusted (mL/min/1.73 m^2)		99.2 (32.8)		96.5 (33.0)		97.3
CrCl	162.0 (34.4)		160.7 (26.3)		99.2	
GFR, Zappitelli	138.5 (15.7)		132.1 (13.0)		95.4	
GFR, Schwartz	112.7 (11.2)		109.6 (10.4)		97.2	

Values reported as mean (standard deviation). The ratio of obese/nonobese was calculated using mean data

BMI body mass index, *BSA* body surface area, *CrCl* creatinine clearance, *FFM* fat-free mass, *LBW* lean body weight

[a]The three reported GFR estimation methods include (1) estimating CrCl through a 24-h urine collection as a surrogate measure of GFR, (2) estimation of GFR using the Zappitelli equation, and (3) estimation of GFR using the Schwartz equation [48, 49]. Simulated GFR is estimated based on each virtual subject's kidney size. Further description and equations for each method are provided in Sect. 1.4 of the ESM

prediction interval (6% above, 40% below) and an AFE of 1.53 (Figs. 12 and 13 of the ESM). No trends were identified that explained model overestimation of observed concentrations (Fig. 12 of the ESM).

3.9.1 Dosing Simulations

Clindamycin, trimethoprim, and sulfamethoxazole weight-normalized clearance decreased with obesity, as increases in absolute clearance attributable to increased kidney volume (thus GFR) in the virtual population of children with obesity did not increase to the same degree as body weight with obesity (Fig. 3, Figs. 14–18 of the ESM). This decreasing trend in weight-normalized clearance was more profound with increasing percent renal elimination. Decreased clearance coupled with higher absolute doses under weight-based dosing resulted in higher AUC_{ss} in virtual children with vs without obesity for all drugs (Figs. 19 and 20 of the ESM). Weight-normalized volume of distribution decreased with obesity as well and was more pronounced with higher lipophilicity and fraction of drug unbound.

All clindamycin dosing simulations resulted in median $AUC_{0-8,ss}$ values within 30% of the adult median, except children aged 2–6 years receiving a fixed adult dose who had higher exposure (58.5% higher than the adult median) (Fig. 4). Simulated exposure when implementing the dose cap of 900 mg was similar to unrestricted recommended dosing, as a minority of children reached the dose cap despite higher body weights (0%, 0.6%, and 26% of virtual children aged > 2–6 years, > 6–12 years, and > 12–18 years, respectively).

Simulations of adult trimethoprim/sulfamethoxazole dosing resulted in nearly all virtual children with obesity aged 2–12 years meeting the target AUC_{ss} and maximum concentration measures for safety and efficacy (Fig. 5). All virtual children with obesity aged 12–18 years met the safety targets for trimethoprim and sulfamethoxazole, but 25.3% of virtual children's trimethoprim AUC_{ss} fell below the target for efficacy. Simulations of recommended pediatric dosing without capping resulted in nearly all virtual children meeting safety and efficacy targets. However, 16.8% and 50.9% of virtual children aged 2–12 years and 12–18 years, respectively, received dosing that exceeded the maximum FDA-recommended adult dose. Further simulations implementing this maximum as a cap resulted in nearly all virtual children in both age groups still meeting safety and efficacy targets.

4 Discussion

We developed a virtual population of children with obesity that accounts for obesity-related physiological changes affecting drug disposition that should be considered for PBPK modeling. Previous adult PBPK modeling by Ghobadi et al. also incorporated obesity-related physiological changes to characterize the disposition of eight drugs [15]. However, physiological changes with obesity in adults cannot simply be extrapolated to children, as for example, studies of CYP3A4-mediated clearance of midazolam in adults vs adolescents show different trends with obesity [38]. Thus, a new virtual population of children with obesity was needed to use PBPK modeling to investigate drug exposure in these children.

To develop a virtual population that better reflects today's obesity prevalence, it was necessary to update the CDC growth curves with the latest demographic data. These updated growth curves are not meant to supplant current measures of obesity, but rather serve as a better description of the body size distribution of today's children of different gender and race in informing the virtual population's body size range. The previous CDC growth curves were developed using observed body sizes of children in the 1980s, when the prevalence of obesity was far lower. In addition to age and sex, the new growth curves also capture racial differences in obesity rates. Note that although the absolute BMI cut-off for obesity has not changed (95th BMI percentile from the original CDC growth curves), the percent of children falling above that cut-off better reflects the current obesity prevalence.

Renal function is challenging to estimate in children with obesity, as there are no studies measuring GFR directly in these children, and there are no GFR equations validated in children with obesity. Extrapolating from studies of GFR in adults with obesity is not reliable, as adults often have comorbidities that cause decreased renal function. While an indirect comparison, reported GFR values from creatinine clearance and GFR estimated by the Zappitelli and Schwartz equations were similar to increased simulated GFR from increased kidney volume in virtual children. Simulated GFR best matched GFR estimated by the Schwartz equation, the most commonly used clinical estimation method for children. This method uses height in addition to creatinine to (indirectly) account for differences in body size in estimating GFR. While reported and simulated absolute GFR is higher in children with vs without obesity, more commonly used standard, or body surface area adjusted, GFR is slightly lower as kidney volume does not increase proportionally to overall increases in body size with obesity.

Literature data describing in vitro changes in metabolic or transporter enzyme activity in children with obesity are lacking, as it is challenging to obtain biopsy samples from these children. Some clinical studies in children with obesity infer changes in metabolic enzyme activity from drug clearance or metabolite formation rate, but these are indirect measures that can be complicated by comorbidities, duration of obesity, or concomitant drug administration. Some important

Fig. 3 Changes in simulated weight-normalized clearance (**a**, **c**, **e**) and weight-normalized volume of distribution (**b**, **d**, **f**) for clindamycin (**a**, **b**), trimethoprim (**c**, **d**), and sulfamethoxazole (**e**, **f**) with increasing body size, i.e., extended body mass index (BMI) percentile. Extended BMI percentile is calculated as BMI divided by the 95th BMI percentile for a subject's age and sex, where children with an extended BMI percentile ≥ 100% are considered obese. Clearance and volume of distribution were calculated from virtual children aged 12–18 years with and without obesity (similar plots for virtual children aged 2–6 years and 6–12 years are presented in Figs. 14 and 15 of the ESM). Virtual children received single doses of 600 mg intravenous (IV) infusion (30 min) clindamycin (CLIN), 160 mg oral (PO) trimethoprim (TMP), and 800 mg PO sulfamethoxazole (SMX). The shaded regions denote the 90% (95th and 5th percentiles), 80% (90th and 10th percentiles), and 50% (75th and 25th percentiles) prediction intervals from lightest to darkest color intensity, respectively. The black line denotes the median prediction. Note that variability in pharmacokinetic parameters appears decreased at the upper extremity of extended BMI percentile owing to a lower number of virtual subjects in this range
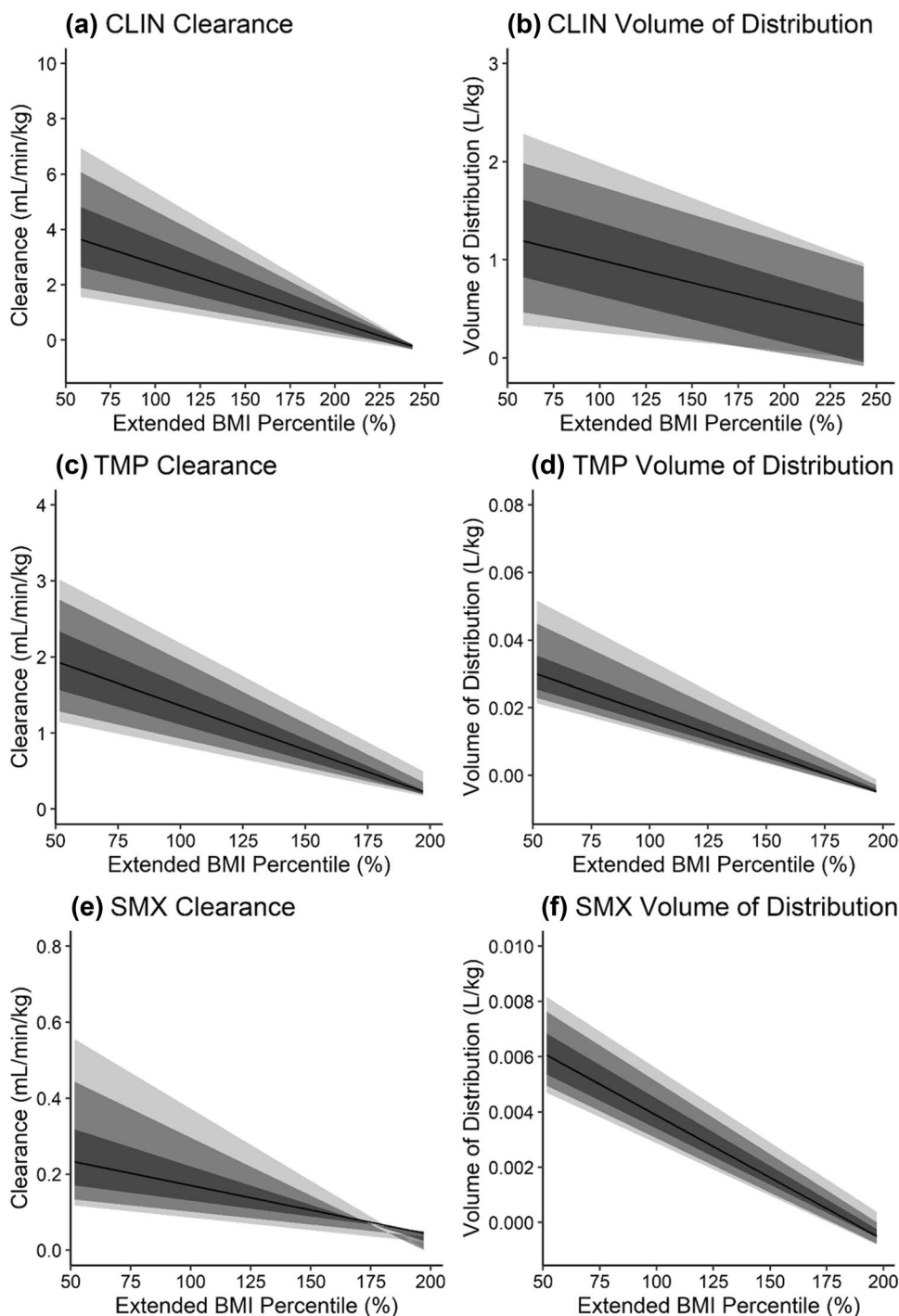
clinical and in vitro studies of adult patients with nonalcoholic steatohepatitis, a common comorbidity of obesity, found substantially altered organic anion transporting polypeptide and multidrug resistance-associated protein transporter activity [39–41]. These changes should be considered when modeling drugs with high transport activity, especially as these transporter changes are explored in children.

Preliminary clindamycin PBPK modeling results in children with obesity showed a clear trend of concentration underestimation with increasing AAG concentrations. Correcting fraction unbound using observed AAG concentrations resulted in strong overall model performance. While limited pediatric AAG literature data did not indicate a trend in increasing AAG concentration with obesity, studies in adults indicate this protein increases with obesity due to inflammation [42, 43]. Thus, exploring a potential increase in AAG concentrations is recommended when evaluating drugs where AAG concentrations strongly impact clearance
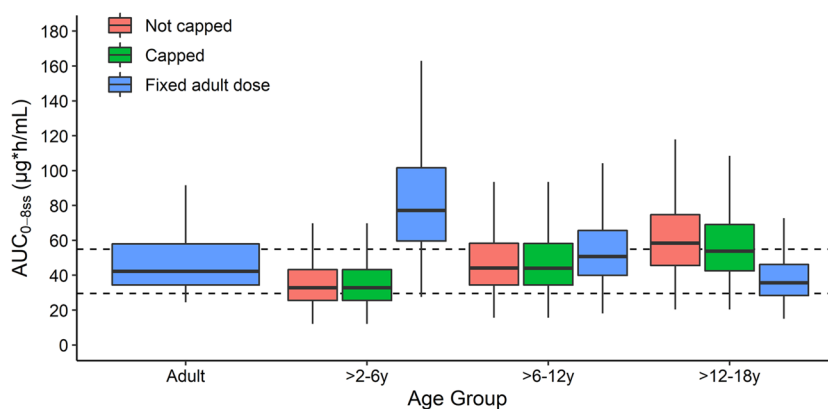
Fig. 4 Boxplots of simulated clindamycin steady-state area under the concentration–time curve from 0 to 8 h ($AUC_{0-8,ss}$) in virtual healthy adults (reference) and virtual children with obesity following population simulations ($n = 1000$ per age group). Adults received the reference clindamycin dose of 600 mg intravenously (IV). Children received either the total weight-based recommended dose (12 mg/kg IV for children aged > 2–6 years and 10 mg/kg IV for children aged > 6–18 years) or the recommended dosing capped at 900 mg IV, or a fixed adult dose of 600 mg IV. Boxes represent the median and interquartile range (IQR), and whiskers extend to 1.5*IQR. Dashed lines represent the $AUC_{0-8,ss}$ range that is within 30% of the adult median $AUC_{0-8,ss}$ value

Fig. 5 Boxplots of simulated trimethoprim (TMP) and sulfamethoxazole (SMX) steady-state area under the concentration–time curve (AUC_{ss}) and maximum concentration (C_{max}) in virtual children with obesity following population simulations ($n = 1000$ per age group). Virtual children received either the total weight-based recommended dose (6 and 30 mg/kg orally [PO] for children aged > 2–12 years and 4 and 20 mg/kg PO for children aged > 12–18 years) or the recommended dosing with a cap of 320 and 1600 mg PO, as per the US Food and Drug Administration (FDA) maximum recommended dose, or a fixed adult dose of 160 and 800 mg PO for TMP and SMX, respectively. Boxes represent the median and interquartile range (IQR), and whiskers extend to 1.5*IQR. The solid line represents the target AUC_{ss} efficacy threshold for TMP, and the dashed lines represent the toxicity AUC_{ss} and C_{max} thresholds for both TMP and SMX
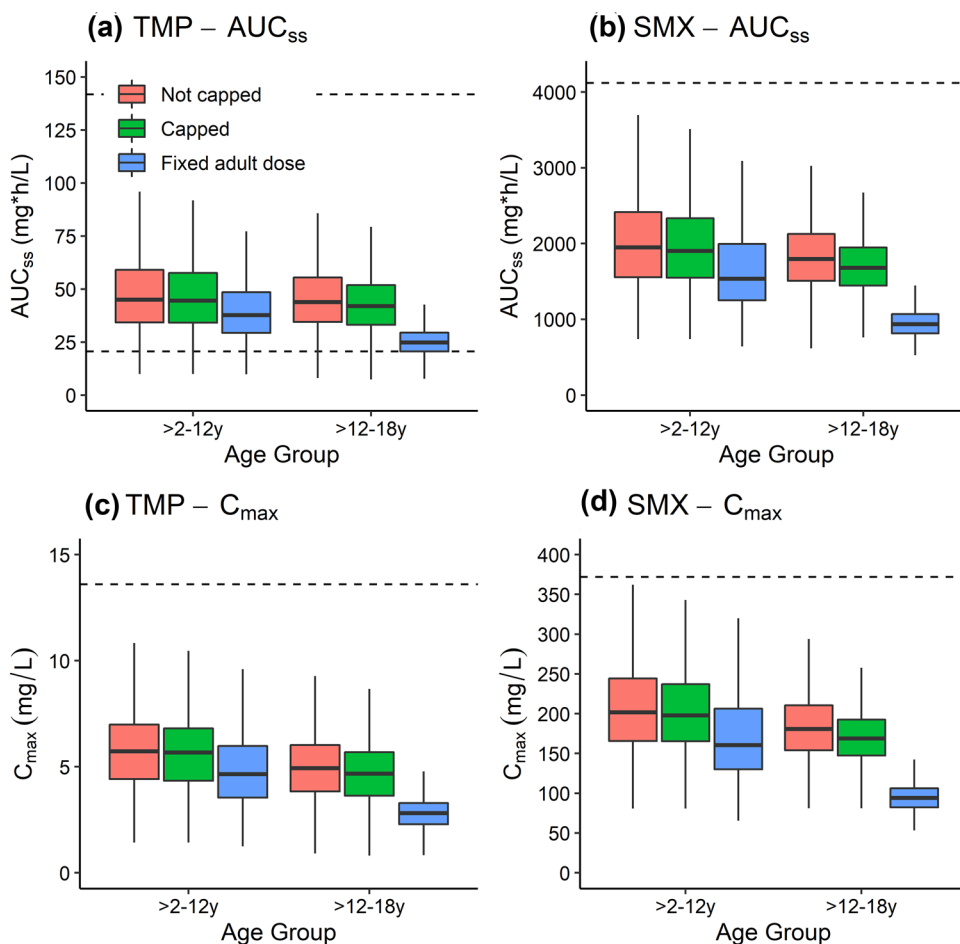
(such as clindamycin) in subjects with obesity. Clindamycin dosing simulations suggest that for children with obesity aged <12 years, recommended pediatric weight-based dosing results in comparable exposure to known efficacious adult exposure (within 25% of the median), even when capping the dose using the FDA maximum. A greater number

of children with obesity aged > 12 years had weight-based dosing that exceeded the FDA maximum, and resulted in significantly higher exposure than the adult median. Thus, PBPK model simulations support current recommended pediatric dosing for children with obesity, with dose capping particularly appropriate for those in older age groups.

Trimethoprim/sulfamethoxazole PBPK modeling in children with obesity resulted in overestimation of sulfamethoxazole concentrations, particularly in the terminal phase. Sulfamethoxazole is ~ 16% cleared by NAT2. While data informing changes in metabolic enzyme activity are limited, one study of caffeine clearance mediated by NAT2 metabolism in children with obesity found that NAT2 activity was five-fold higher in these children compared with normal weight controls [44]. Incorporating this increase in NAT2 clearance into the PBPK model resulted in substantially better model performance (AFE of 0.93 for sulfamethoxazole, Fig. 21 of the ESM), further supporting the theory that NAT2 activity is increased in children with obesity. Further studies of drugs metabolized by NAT2 in patients with obesity should explore this potential increase in clearance. Dosing simulations revealed that all children with obesity aged < 12 years met the efficacy and safety targets for both drugs, regardless of using the full recommended pediatric weight-based dose, or capping based on the FDA maximum or adult dose. The same was true for children with obesity aged > 12 years, except fixing the dose to the recommended adult dose resulted in underexposure for more than a quarter of virtual children. Thus, the recommended pediatric weight-based dosing capped with the FDA maximum should be used for older age groups.

This is the first virtual population that mechanistically describes children with obesity, and the first PBPK modeling in this patient population. However, this work is not without limitations. In some cases, limited data were available to inform the physiological assumptions in the virtual population. Data were not available to inform a more gradual effect of physiological changes from children without vs with obesity (i.e., changes affecting children with overweight). While racial differences were accounted for in body size by the updated growth curves, data to inform these differences for other physiological parameters in the virtual population are lacking. Important future work will need to be conducted as more physiological information in minority groups becomes available to fully understand how differing obesity prevalence might affect dosing in these groups. The changes in pharmacokinetic parameters induced by obesity may be more pronounced in these patient populations. Additionally, data sources were derived from different patient populations (e.g., healthy volunteers from NHANES vs inpatient children from the PTN Data Repository), and thus may not be directly comparable. At present, only three drugs have been used to evaluate the virtual population, all of which have similar lipophilicities and volumes of distribution. The three drugs presented herein do not represent the full spectrum of drugs dosed in children with obesity. For the many drugs that are more lipid soluble, the degree of obesity is likely to have a far greater impact on the volume of distribution as previously demonstrated in adults [45–47]. The underlying PBPK models used to apply the virtual population were developed using sparse data in children without obesity, and it is difficult to attribute any bias in pediatric obese predictions to the underlying PBPK model or the novel virtual population. It is important to note that the virtual population of children in its current form is intended as an important first step in enabling PBPK modeling for this vulnerable patient population. It should be viewed as a starting point to which a new physiologic understanding of obesity can be added as it becomes available.

5 Conclusions

In this study, a virtual population of children with obesity was developed that incorporates obesity-related physiological changes to enable PBPK modeling. This virtual population was evaluated by successfully predicting the PK of clindamycin and trimethoprim\sulfamethoxazole in children with obesity by using published PBPK models that were previously evaluated in non-obese children. Model simulations support current recommended pediatric dosing for all three drugs as these regimens achieved target exposure in children with obesity with or without dose capping, despite decreased weight-normalized clearance and higher absolute doses under weight-based dosing. While confirmatory of prior dosing recommendations in these cases, this novel virtual population can be applied to other drugs to better understand dosing in children with obesity.

Declarations

Conflict of Interest/Competing Interests M.C.-W. received support from the NICHD (HHSN275201000003I), the National Center for Advancing Translational Sciences [1U24TR001608]), and the FDA (1U18FD006298); he also receives research support from industry for neonatal and pediatric drug development, https://dcri.org/about-us/conflict-of-interest/. The remaining authors have no relevant conflicts of interest to disclose.

Ethics Approval The original studies that facilitated the collection of the clindamycin and trimethoprim/sulfamethoxazole data were institutional review board approved. No new subject enrollment took place as part of this study. The PBPK modeling research was institutional review board approved at the University of North Carolina at Chapel Hill.

Consent to Participate Informed consent and assent, when applicable, were obtained from all participants enrolled in the original studies that facilitated the collection of the clindamycin and trimethoprim/sulfamethoxazole data who contributed clinical pharmacokinetic data used in this study.

Consent for Publication Not applicable.

Code Availability The open-source PBPK platform PK-Sim® was used, as described in this manuscript.

Availability of Data and Material Clindamycin and trimethoprim/sulfamethoxazole pharmacokinetic data collected by the Pediatric Trials Network were accessed through the NICHD Data and Specimen Hub (DASH, https://dash.nichd.nih.gov/). To help expand the knowledge base for pediatric medicine, the PTN is pleased to share data from its completed and published studies with interested investigators. For requests, please contact: PTN-Program-Manager@dm.duke.edu.

Authors' Contributions Participated in research design: J.G.G., A.N.E., and D.G. Performed the data analysis: J.G.G., F.O.C., J.S., S.G., and V.H. Wrote or contributed to the writing of the manuscript: J.G.G., F.O.C., A.N.E., J.S., E.M.P., K.R.K., A.R., C.P.H., V.H., S.G., M.C.W, and D.G.

References

1. Skinner AC, Ravanbakht SN, Skelton JA, Perrin EM, Armstrong SC. Prevalence of obesity and severe obesity in US children, 1999–2016. Pediatrics. 2018;141: e20173459.
2. World Health Organization. Report of the commision on ending childhood obesity. WHO Doc Prod Serv. 2016. https://apps.who.int/iris/bitstream/handle/10665/204176/9789241510066_eng.pdf;sequence=1. Accessed 14 Nov 2020.
3. (NCD-RisC) NRFC. Worldwide trends in body-mass index, underweight, overweight, and obesity from 1975 to 2016: a pooled analysis of 2416 population-based measurement studies in 128.9 million children, adolescents, and adults. Lancet. 2017;390:2627–42.
4. Solmi F, Morris S. Association between childhood obesity and use of regular medications in the UK: longitudinal cohort study of children aged 5–11 years. BMJ Open. 2015;5: e007373.
5. Vernacchio L, Kelly JP, Kaufman DW, Mitchell AA. Medication use among children < 12 years of age in the United States: results from the Slone Survey. Pediatrics. 2009;124:446–54.
6. Vaughns JD, Conklin LS, Long Y, Zheng P, Faruque F, Green DJ, et al. Obesity and pediatric drug development. J Clin Pharmacol. 2018;58:650–61.
7. Hanley MJ, Abernethy DR, Greenblatt DJ. Effect of obesity on the pharmacokinetics of drugs in humans. Clin Pharmacokinet. 2010;49:71–87.
8. Brill MJE, Diepstraten J, van Rongen A, van Kralingen S, van den Anker JN, Knibbe CAJ. Impact of obesity on drug metabolism and elimination in adults and children. Clin Pharmacokinet. 2012;51:277–304.
9. Cheymol G. Effects of obesity on pharmacokinetics: implications for drug therapy. Clin Pharmacokinet. 2000;39:215–31.
10. Harskamp-van Ginkel MW, Hill KD, Becker K, Testoni D, Cohen-Wolkowiez M, Gonzalez D, et al. Drug dosing in obese children: a systematic review of current pharmacokinetic data. J Am Med Assoc Pediatr. 2015;169:678–85.
11. Cleocin Phosphate® (clindamycin injection, USP) and (clindamycin injection in 5% dextrose). https://www.accessdata.fda.gov/drugsatfda_docs/label/2008/050441s055,050639s016lbl.pdf. Accessed 14 Nov 2020.
12. Cao Y, Jusko WJ. Applications of minimal physiologically-based pharmacokinetic models. J Pharmacokinet Pharmacodyn. 2012;39:711–23.
13. Kuepfer L, Niederalt C, Wendl T, Schlender JF, Willmann S, Lippert J, et al. Applied concepts in PBPK modeling: how to build a PBPK/PD model. CPT Pharmacomet Syst Pharmacol. 2016;5:516–31.
14. Barrett JS, della Alberighi OC, Läer S, Meibohm B. Physiologically based pharmacokinetic (PBPK) modeling in children. Clin Pharmacol Ther. 2012;92:40–9.
15. Ghobadi C, Johnson TN, Aarabi M, Almond LM, Allabi AC, Rowland-Yeo K, et al. Application of a systems approach to the bottom-up assessment of pharmacokinetics in obese patients: expected variations in clearance. Clin Pharmacokinet. 2011;50:809–22.
16. Edginton AN, Schmitt W, Willmann S. Development and evaluation of a generic physiologically based pharmacokinetic model for children. Clin Pharmacokinet. 2006;45:1013–34.

17. Hornik CP, Wu H, Edginton AN, Watt K, Cohen-Wolkowiez M, Gonzalez D. Development of a pediatric physiologically-based pharmacokinetic model of clindamycin using opportunistic pharmacokinetic data. Clin Pharmacokinet. 2017;56:1343–53.

18. Thompson EJ, Wu H, Maharaj A, Edginton AN, Balevic SJ, Cobbaert M, et al. Physiologically based pharmacokinetic modeling for trimethoprim and sulfamethoxazole in children. Clin Pharmacokinet. 2019;58:887–98.

19. Centers for Disease Control and Prevention (CDC). National Center for Health Statistics (NCHS). National Health and Nutrition Examination Survey Data. Hyattsville, MD: US Department of Health and Human Services, Centers for Disease Control and Prevention. https://www.cdc.gov/nchs/nhanes/index.htm. Accessed 25 Oct 2019.

20. Hornik CP, Atz AM, Bendel C, Chan F, Downes K, Grundmeier R, et al. Creation of a multicenter pediatric inpatient data repository derived from electronic health records. Appl Clin Inform. 2019;10:307–15.

21. Smith MJ, Gonzalez D, Goldman JL, Yogev R, Sullivan JE, Reed MD, et al. Pharmacokinetics of clindamycin in obese and non-obese children. Antimicrob Agents Chemother. 2017;61:1–12.

22. Gonzalez D, Delmore P, Bloom BT, Cotten CM, Poindexter BB, McGowan E, et al. Clindamycin pharmacokinetics and safety in preterm and term infants. Antimicrob Agents Chemother. 2016;60:2888–94.

23. Gulati AK, Kaplan DW, Daniels SR. Clinical tracking of severely obese children: a new growth chart. Pediatrics. 2012;130:1136–40.

24. Autmizguine J, Melloni C, Hornik CP, Dallefeld S, Harper B, Yogev R, et al. Population pharmacokinetics of trimethoprim-sulfamethoxazole in infants and children. Antimicrob Agents Chemother. 2018;62:1–19.

25. Gonzalez D, Melloni C, Yogev R, Poindexter BB, Mendley SR, Delmore P, et al. Use of opportunistic clinical data and a population pharmacokinetic model to support dosing of clindamycin for premature infants to adolescents. Clin Pharmacol Ther. 2014;96:429–37.

26. Wu YSS, Cohen-Wolkowiez M, Hornik CP, Gerhart JG, Autmizguine J, Cobbaert M, et al. External evaluation of two pediatric population pharmacokinetics models of oral trimethoprim and sulfamethoxazole. Antimicrob Agents Chemother. 2021;65(7): e0214920.

27. Liu C, Bayer A, Cosgrove SE, Daum RS, Fridkin SK, Gorwitz RJ, et al. Clinical practice guidelines by the Infectious Diseases Society of America for the treatment of methicillin-resistant *Staphylococcus aureus* infections in adults and children: executive summary. Clin Infect Dis. 2011;52:285–92.

28. Kremers P, Duviver J, Heusghem C. Pharmacokinetic studies of co-trimoxazole in man after single and repeated doses. J Clin Pharmacol. 1974;14:112–7.

29. Stevens RC, Laizure SC, Sanders PL, Stein DS. Multiple-dose pharmacokinetics of 12 milligrams of trimethoprim and 60 milligrams of sulfamethoxazole per kilogram of body weight per day in healthy volunteers. Antimicrob Agents Chemother. 1993;37:448–52.

30. Bactrim (sulfamethoxazole and trimethoprim) injection, for intravenous use. https://www.accessdata.fda.gov/drugsatfda_docs/label/2017/018374s025lbl.pdf. Accessed 14 Nov 2020.

31. Kuczmarski RJ, Ogden CL, Guo SS, Grummer-Strawn LM, Flegal KM, Mei Z, et al. 2000 CDC growth charts for the United States: methods and development. Vital Health Stat. 2002;246:1–190.

32. Hwaung P, Bosy-Westphal A, Muller MJ, Geisler C, Heo M, Thomas DM, et al. Obesity tissue: composition, energy expenditure, and energy content in adult humans. Obesity. 2019;27:1472–81.

33. Al-Sallami HS, Goulding A, Grant A, Taylor R, Holford N, Duffull SB. Prediction of fat-free mass in children. Clin Pharmacokinet. 2015;54:1169–78.

34. Green TP, Binns HJ, Wu H, Ariza AJ, Perrin EM, Quadri M, et al. Estimation of body fat percentage for clinical pharmacokinetic studies in children. Clin Transl Sci. 2021;14(2):509–17.

35. Correia-Costa L, Schaefer F, Afonso AC, Bustorff M, Guimarães JT, Guerra A, et al. Normalization of glomerular filtration rate in obese children. Pediatr Nephrol. 2016;31:1321–8.

36. Krogstad V, Peric A, Robertsen I, Kringen MK, Vistnes M, Hjelmesæth J, et al. Correlation of body weight and composition with hepatic activities of cytochrome P450 enzymes. J Pharm Sci. 2021;110:432–7.

37. Ulvestad M, Skottheim IB, Jakobsen GS, Bremer S, Molden E, Åsberg A, et al. Impact of OATP1B1, MDR1, and CYP3A4 expression in liver and intestine on interpatient pharmacokinetic variability of atorvastatin in obese subjects. Clin Pharmacol Ther. 2013;93:275–82.

38. van Rongen A, Brill MJE, Vaughns JD, Valitalo PAJ, van Dongen EPA, van Ramshorst B, et al. Higher midazolam clearance in obese adolescents compared with morbidly obese adults. Clin Pharmacokinet. 2018;57:601–11.

39. Ali I, Slizgi JR, Kaullen JD, Ivanovic M, Niemi M, Stewart PW, et al. Transporter-mediated alterations in patients with NASH increase systemic and hepatic exposure to an OATP and MRP2 substrate. Clin Pharmacol Ther. 2018;104(4):749–756. https://doi.org/10.1002/cpt.997.

40. Pierre V, Johnston CK, Ferslew BC, Brouwer KLR, Gonzalez D. Population pharmacokinetics of morphine in patients with nonalcoholic steatohepatitis (NASH) and healthy adults. CPT Pharmacomet Syst Pharmacol. 2017;6:331–9.

41. Sjöstedt N, Neuhoff S, Brouwer KLR. Physiologically-based pharmacokinetic model of morphine and morphine-3-glucuronide in nonalcoholic steatohepatitis. Clin Pharmacol Ther. 2021;109:676–87.

42. Benedek I, Fiske W III, Griffen W, Bell R, Blouin R, McNamara P. Serum α1-acid glycoprotein and the binding of drugs in obesity. Br J Clin Pharmacol. 1983;16:751–4.

43. Benedek I, Blouin R, McNamara P. Serum protein binding and the role of increased α1-acid glycoprotein in moderately obese male subjects. Br J Clin Pharmacol. 1984;18:941–6.

44. Chiney MS, Schwarzenberg SJ, Johnson LA. Altered xanthine oxidase and N-acetyltransferase activity in obese children. Br J Clin Pharmacol. 2011;72:109–15.

45. Smit C, de Hoogd S, Brüggemann RJM, Knibbe CAJ. Obesity and drug pharmacology: a review of the influence of obesity on pharmacokinetic and pharmacodynamic parameters. Expert Opin Drug Metab Toxicol. 2018;14:275–85.

46. Abernethy DR, Greenblatt DJ. Drug disposition in obese humans: an update. Clin Pharmacokinet. 1986;11:199–213.

47. Bruno CD, Harmatz JS, Duan SX, Zhang Q, Chow CR, Greenblatt DJ. Effect of lipophilicity on drug distribution and elimination: influence of obesity. Br J Clin Pharmacol. 2021;8(87):3197–205.

48. Zappitelli M, Parvex P, Joseph L, Paradis G, Grey V, Lau S, et al. Derivation and validation of cystatin C-based prediction equations for GFR in children. Am J Kidney Dis. 2006;48:221–30.

49. Schwartz GJ, Muñoz A, Schneider MF, Mak RH, Kaskel F, Warady BA, et al. New equations to estimate GFR in children with CKD. J Am Soc Nephrol. 2009;20:629–37.

Authors and Affiliations

Jacqueline G. Gerhart[1] · Fernando O. Carreño[1] · Andrea N. Edginton[2] · Jaydeep Sinha[1] · Eliana M. Perrin[3] · Karan R. Kumar[4,5] · Aruna Rikhi[4] · Christoph P. Hornik[4,5] · Vincent Harris[1] · Samit Ganguly[1,6] · Michael Cohen-Wolkowiez[4,5] · Daniel Gonzalez[1] ⓘ **on behalf of the Best Pharmaceuticals for Children Act— Pediatric Trials Network Steering Committee**

[1] Division of Pharmacotherapy and Experimental Therapeutics, UNC Eshelman School of Pharmacy, The University of North Carolina at Chapel Hill, 301 Pharmacy Lane, Campus Box #7569, Chapel Hill, NC 27599-7569, USA

[2] School of Pharmacy, University of Waterloo, Waterloo, ON, Canada

[3] Department of Pediatrics, School of Medicine and School of Nursing, Johns Hopkins University, Baltimore, MD, USA

[4] Duke Clinical Research Institute, Durham, NC, USA

[5] Department of Pediatrics, Duke University School of Medicine, Durham, NC, USA

[6] Regeneron Pharmaceuticals, Inc., Tarrytown, NY, USA